Energy 269 (2023) 126821

Contents lists available at ScienceDirect

Energy

journal homepage: www.elsevier.com/locate/energy

Carbon dioxide and acetone mixtures as refrigerants for industry heat pumps to supply temperature in the range 150–220 °C

J. Gómez-Hernández [a,*], R. Grimes [b], J.V. Briongos [a], C. Marugán-Cruz [a], D. Santana [a]

[a] Energy Systems Engineering Group (ISE), Department of Thermal and Fluid Engineering, Universidad Carlos III de Madrid, Av. Universidad, 30, 28911, Leganés, Madrid, Spain
[b] Stokes Laboratories, Bernal Institute, School of Engineering, University of Limerick, Ireland

ARTICLE INFO

Handling Editor: Yunho Hwang

Keywords:
Industry decarbonization
High temperature heat pumps
Heat upgrade
Carbon dioxide
Acetone
Zeotropic refrigerant

ABSTRACT

Industry decarbonization is a key a challenge towards the transition to climate neutrality. Indeed, there is a need to satisfy heat at temperatures higher than 150 °C in relevant industrial sectors by upgrading lower temperature heat flows, such as heat from renewable heat sources, ambient heat or industrial waste heat. High temperature heat pumps (HTHP) can upgrade such heat flows enabling great savings in carbon emissions. New refrigerants are needed to develop HTHPs achieving high performances at high temperatures. This paper proposes the use of a new zeotropic mixture composed of carbon dioxide and acetone as the refrigerant of HTHPs working in the temperature range of 150–220 °C. The new fluid is compared with existing pure refrigerants currently used. The thermodynamic characterization of the CO_2/acetone mixtures shows temperature glides below 50 K for CO_2 mass fractions up to 10%. The best HTHP performance is shown for the mixture 5% CO_2/95% acetone in mass fraction. For instance, such a mixture obtains a COP of 5.63 when the target outlet sink temperature is 200 °C and the temperature difference between the outlet heat sink and the inlet heat source is 70 K, showing an improvement of 46% compared to pure acetone.

1. Introduction

In 2021, heating in industrial processes accounted for approximately 25% of global energy consumption [1]. Most of this heat is provided using fossil fuels – in the EU for example gas, oil and coal provide 42%, 12% and 8% of heat respectively. Only 13% of process heat in the EU is provided by renewable sources, 11% of this being provided by biomass. Electricity provides 12% of the EU's process heat – some of this may be renewable, depending on the local power generation mix. Heat pumps provide only 1% of the EU's process heat [2]. Because such a low fraction of global process heat is provided by renewable energy sources, carbon emissions are very high, estimated at 7.5 Gt globally in 2016, approximately one fifth of all global CO_2 emissions [3].

The requirements of heat across industrial sectors are diverse, and the range of temperatures at which heat is provided varies significantly between industrial sectors. Food processing industries for example require heat at temperatures only marginally higher than ambient, chemical and petrochemical industries consume significant quantities of heat in the range of 200–500 °C, and the cement and steel industries require heat at temperatures in excess of 1500 °C [4]. Because of the diversity in process heat requirements, it is unlikely that any one solution will emerge to decarbonise industrial process heat, but rather a range of solutions with specific technologies providing solutions to specific applications.

In recent years, there has been substantial growth in the share of renewable electricity production on many electrical grids. As the share of renewable electricity production grows, a trend towards electrification of many energy demands is developing. In the EU, electrification of heating across all sectors is seen as a key part of the decarbonization of heat [5]. In some instances electrification of heating will entail Ohmic heating, but where the required heat supply temperatures are appropriate, the use of heat pumps will enable much greater savings in carbon emissions.

A large proportion of industrial process heat is unused, and rejected as waste heat. In the EU it was estimated in 2013 that 20–30% of process heat was lost in the form of waste heat [6]. This waste heat is rejected over a diverse range of temperatures. High temperature waste heat can be readily used for generation of power using a Rankine cycle, or to provide heat to other processes within a processing facility. Lower temperature waste heat may also be used, for example in district heating, however such uses of low-grade waste heat are dependent upon

* Corresponding author.
E-mail address: jegomez@ing.uc3m.es (J. Gómez-Hernández).

https://doi.org/10.1016/j.energy.2023.126821
Received 7 June 2022; Received in revised form 28 November 2022; Accepted 26 January 2023
Available online 28 January 2023

Nomenclature

Abbreviations

COP	coefficient of performance
GWP	global warming potential
HTF	heat transfer fluid
HTHP	high temperature heat pump
IHX	internal heat exchanger
NBP	normal boiling point
ODP	ozone depletion potential
RPM	revolutions per minute
SG	safety group classification
VHC	volumetric heating capacity

Symbols

h	enthalpy
$\dot{m}$	mass flow rate
P	pressure
$\dot{Q}$heat rate$s$	heat ratesentropy
T	temperature
$\overline{T}$	thermodynamic average temperature
ΔTtemperature differenceΔT_{lift}	temperature lift between the condenser and the evaporator$x$ temperature differenceΔT_{lift}temperature lift between the condenser and the evaporator$x$quality
VHC	volumetric heating capacity

$\dot{W}$power*Greek symbols*

Δ*difference*η	*difference*ηisentropic efficiency
ρ	density

πpressure *ratioSubscripts*

100	100-year time horizon
bub	bubble point
cond	condenser
comp	compressor
crit	critical
dew	dew point
evap	evaporator
i	inlet
Lor	Lorenz
loss	losses
max	maximum
o	outlet
pinch	pinch point
sat	saturated
SC	subcooled
SH	superheated
sink	heat sink
source	heat source

demand for heat being in close proximity to the facility where it is generated.

The total waste heat potential in the EU is estimated at 304.13 TWh/year. Waste heat potential at temperatures in the range of 100–200 °C is high, about 100 TWh/year, representing approximately one third of the overall waste heat potential [6]. This is available in a large variety of industrial sectors. The use of a heat pump to upgrade the heat in these waste heat streams to temperatures of 50–70 °C higher would enable heat delivery to processes at temperatures in the range of 150 °C–250 °C [7,8]. Data from Australia indicates that approximately 38% of industrial process heat requirements are in this temperature range [9]. Several industrial processes could integrate the heat pumps at high temperatures, such as drying, pasteurization, sterilization, steam generation, papermaking, food preparation [10,11]. Assuming sufficiently high Coefficients of Performance (COP) such heat pumps could significantly reduce energy consumption. If such heat pumps are used in regions with a high mix of renewable electricity generation, the carbon emissions could be significantly reduced.

There is a clear need of developing high temperature heat pumps (HTHP) for industry processes with heat sink temperatures above 100 °C [12–16]. The harsh industrial requirements, the variety of applications, the high reliability, the high temperatures and the environmental impact of current refrigerants have difficulted the integration of HTHPs in industry. In this way, to meet the industry standards, new HTHP developments should increase efficiency, resist high temperatures in all components and use environmentally friendly refrigerants with low Global Warming Potential (GWP) and low Ozone Depletion Potential (ODP) [10].

The refrigerant properties play a fundamental role in the HTHP performance. The selection of the refrigerant is mainly performed attending to their thermodynamic properties, toxicity, flammability, environmental footprint (ODP and GWP) and costs. Current trends for HTHPs focus on developing new refrigerants with low GWP and ODP at temperatures of 150–250 °C. HTHP technologies that supply a heat sink temperature of 160 °C are already available at the market. In particular, Kobelco SGH 165 heat pump employs a twin-screw compressor reaching a sink temperature of 165 °C, showing COP values of 2.2 for a temperature difference between the condenser and the evaporator of 105 °C [17]. The refrigerant R245fa, employed in Kobelco SGH 165, is the dominant refrigerant in the temperature range of 120–150 °C [16]. However, it has a high environmental impact with a GWP of 858. To overcome this environmental limitation, the refrigerant HCFO-1224yd (Z) has been recently proposed as a low-GWP substitute of R245fa [18]. Other works have explored the use of R718 as refrigerant in a HTHP prototype reaching condensation temperatures of 130 °C with a COP of 3.1 for a temperature lift of 50 K [19]. Pure refrigerants with low GWP are screened in Ref. [20] considering their thermo-physical properties, environmental impact, flammability, health-hazard and instability, and effect on the compressor choice. Overall, acetone, benzene, cyclopentane and dichloroethane are recommended as a function of the heat source and heat sink temperatures. However, the application of these refrigerants depends on whether or not the HTHP performance surpasses their risks associated to the toxicity and/or flammability.

Pure refrigerants exhibit a non-zeotropic behavior, meaning that the phase change during constant pressure occurs at constant temperature. An opposite behavior is shown by zeotropic fluids, which present a non-constant temperature during the phase change, which is called the temperature glide. This temperature glide is defined as the difference between the dew point and the bubble point temperatures at constant pressure. The temperature glide is a key parameter to, on the one hand, design both the evaporator and the condenser, and on the other hand, match the source and sink temperature changes to minimize the irreversibilities produced in the heat exchangers [21,22]. Therefore, the refrigerant can be tailored to obtain benefits in the heat pump efficiency depending on the application [23].

Pure fluids can be mixed resulting in new refrigerants characterized by a zeotropic behavior. These zeotropic working fluids have shown improvements in several applications, such as Organic Rankine Cycles [24], power cycles [25], supercritical power cycles [26], and heat pumps [23,27,28]. Concerning HTHPs, the use of zeotropic mixtures can contribute to increase the system performance if there is a good match between the refrigerant and both the sink and source fluids [23]. This would reduce the exergy destruction due to heat transfer. However, the condensation process of a zeotropic mixture is driven by the vapor

pressure of the components. The less volatile component condenses at the dew point temperature, while the more volatile component accumulates at the interface of the liquid condensate and vapor [29]. This changes the composition of the mixture at the interface, producing a concentration gradient that introduces an additional mass transfer and heat transfer resistance compared to a pure fluid condensation process. To overcome this limitation, heat exchangers with zeotropic fluids may require increased heat transfer area. The degree to which the heat exchanger area would need to be increased could be offset by improving the mass and heat transfer coefficients by increasing the mixing between both phases during condensation [22,29].

Despite the improvements shown, there is still a lack of HTHP refrigerants with high performance that are environmentally friendly for temperatures larger than 150 °C. This work proposes a new zeotropic mixture composed by carbon dioxide and acetone as refrigerant of HTHPs to achieve high performances taking advantage of the temperature glide effect. This binary mixture is a zeotropic fluid which properties depend on the CO_2 and acetone contents. On the one hand, carbon dioxide is a natural refrigerant, non-toxic, with low effective GWP and zero ODP that is, for instance, developed for HTHPs for *trans*-critical operation [30]. Its low critical temperature (30.98 °C) makes difficult the subcritical application [31]. On the other hand, acetone is a solvent that belongs to the ketones group, showing high critical temperature (234.95 °C), high flammability, GWP <1 and zero ODP [20]. The CO_2/acetone mixture has been studied for reducing emissions by capturing CO_2 [32], as solvent with sCO_2 [33], and for compression/resorption refrigeration systems [34]. In this regard, air-conditioning application is considered in Ref. [34] for a chilled water temperature of 15 °C, reaching mixture compositions of 50% CO_2 in mass fraction. Therefore, acetone might act as a CO_2 solvent, ensuring good miscibility between both pure fluids, and combining the good thermal properties of CO_2 with the high critical temperature of acetone.

This paper explores the thermodynamic performance of a new refrigerant. Therefore, to simplify the analysis, a single-stage cycle with internal heat-exchanger is employed following the work of [10]. The reader is referred to the literature to analyze the influence of the configuration on the HTHP performance [11,15,35]. Regarding the HTHP components, the compressor is the component with more difficulties to resist the high temperatures [36]. The superheating at the compressor outlet is generally limited up to 180 °C to avoid the thermal decomposition of the compressor lubricant [20,37,38]. However, such a technical constraint may be overcome using oil-free centrifugal compressors [20,39].

This work analyzes the use of the binary mixtures composed by CO_2 and acetone as refrigerant of HTHP for high temperature applications. The thermodynamic properties of the binary mixture are studied as a function of the mixture composition. A single-stage heat pump with internal heat exchanger is modelled to compare the new fluid with existing pure fluid refrigerants. The coefficient of performance, the volumetric heating capacity, the pressure ratio between evaporator and condenser, and the maximum temperature at the compressor outlet are studied for different cases to evaluate the HTHP performance. The results are presented as a function of the temperature lift between condenser and evaporator, and as a function of the temperature difference between the heat sink and source. In all considered cases, the zeotropic mixture with mass fractions of 5% CO_2/95% acetone shows encouraging improvements compared to pure refrigerants.

2. Methods

This section describes the main thermodynamic properties and assumptions used to model the HTHP employing pure fluids (ethanol, methanol, R1233zd(E), R245fa and R600), and CO_2/acetone mixtures as refrigerants. Two heat pump layouts are presented for pure fluids and for CO_2/acetone mixtures. In both layouts, waste heat is assumed to be recovered for supplying the source heat in the evaporator. Furthermore, subcritical operation is considered. The refrigerant temperatures in the HTHP are calculated as a function of two parameters: (i) the temperature lift (ΔT_{lift}) between the condenser and the evaporator, and (ii) the temperature difference between the outlet sink temperature and the inlet source temperature ($\Delta T_{sink,o-source,i}$). Both ΔT_{lift} and $\Delta T_{sink,o-source,i}$ are the main parameters used to compare the thermodynamic efficiency of the presented heat pumps working for pure fluids and CO_2/acetone mixture.

2.1. Refrigerant properties

The refrigerants can be categorized into azeotropic fluids and zeotropic fluids. Azeotropic fluids show a constant temperature during a phase change at constant pressure. The pure refrigerants considered in this work (acetone, ethanol, methanol, R1233zd(E), R245fa and R600) are identified as azeotropic fluids. These pure refrigerants have been studied in HTHPs for working at temperatures above 150 °C [20]. Zeotropic fluids are distinguished by a non-constant temperature during a phase change at constant pressure. Carbon dioxide and acetone mixture present a zeotropic behavior, as it will be seen in the next sections.

Table 1 presents the properties of the pure fluids considered in this work. Regarding the proposed new refrigerant, CO_2/acetone mixture, different compositions are analyzed to determine its performance as refrigerant of a heat pump for high temperature applications. In this sense, several works have published vapor-liquid equilibrium data for the CO_2/acetone mixture. Only the work of [34] presents results for temperatures of 27–77 °C in a pressure range of 1–40 bar and a mass fraction of 50% CO_2, which conditions are near to the studied in this paper. Thus, no experimental data is available for both the temperature and the pressure ranges considered in this work [33]. This lack of experimental data makes necessary to review the literature to predict the behavior of the proposed mixture. As stated in Ref. [40], the availability of the CO_2/acetone mixture can be determined by the miscibility of the mixture and the non-reaction of the two-fluids. On the one hand, carbon dioxide shows good miscibility and good solubility in acetone, as shown in Refs. [33,41,42]. On the other hand, no reactivity is expected for CO_2 and acetone [43]. Therefore, good miscibility between both fluids is assumed in this work.

2.2. Heat pump layout

The main objective of this study is to determine the performance of the proposed CO_2/acetone mixture working as the refrigerant fluid of a heat pump cycle for high temperature applications in industry. To this aim, this paper is focused on the thermodynamic analysis between different pure refrigerants (Table 1) and the CO_2/acetone mixture. Therefore, only simple cycle layouts are analyzed, as shown in Fig. 1-a for pure fluids and in Fig. 1-b for the CO_2/acetone mixture.

Fig. 1-a shows a simple heat pump design used to study pure refrigerants, which is based on [10,51]. An internal heat exchanger is employed to ensure dry compression (state 1). After the compression (state 2), superheated vapor transfers heat to the heat sink ($\dot{Q}_{sink}$) until subcooled liquid state is reached (state 3). Subcooling of 5 K ($\Delta T_{SC} = 5\,K$) is implemented at the condenser outlet. This liquid is further subcooled (state 4), in the internal heat exchanger (IHX) to superheat the evaporator outlet by 5 K (state 6), and throttled to the evaporator pressure (state 5). The evaporation process is assumed to be performed by waste heat from industry applications. Fig. 2 shows the temperature-heat diagram using pure fluids as HTF.

Fig. 1-b proposes the heat pump design used to analyze different CO_2/acetone mixtures. Similarly to the standard heat pump cycle (Fig. 1-a), Fig. 1-b includes an IHX to ensure dry compression. However, the zeotropic behavior of the CO_2/mixture makes it necessary to incorporate some modifications compared to the standard cycle. The

Table 1
Technical and physical properties of the selected working fluids. T_{crit}: critical temperature, P_{crit}: critical pressure, NBP: normal boiling point [44,45], GWP_{100}: Global Warming Potential for 100-year time horizon (basis CO_2 = 1.0 [46,47]), ODP: Ozone Depletion Potential [48], Health and Flammability [49], SG: safety group classification [43,50].

Refrigerant	T_{crit} [°C]	P_{crit} [bar]	NBP [°C]	GWP_{100} [-]	ODP [−]	Health hazard	Flammability	ASHRAE SG
Acetone	234.95	46.92	56.07	0.5	0	1	3	N/A
Carbon dioxide	30.98	73.77	−78.46[a]	1	0	2	0	A1
Ethanol	241.56	62.68	78.42	1	0	2	3	N/A
Methanol	239.45	81.03	64.48	2.8	0	1	3	N/A
R1233zd(E)	166.45	36.24	18.26	1	0	N/A	0	A1
R245fa	153.86	36.51	15.05	858	0	2	1	B1
R600	151.98	37.96	−0.49	4	0	0	4	A3

[a] Normal Sublimation Point.

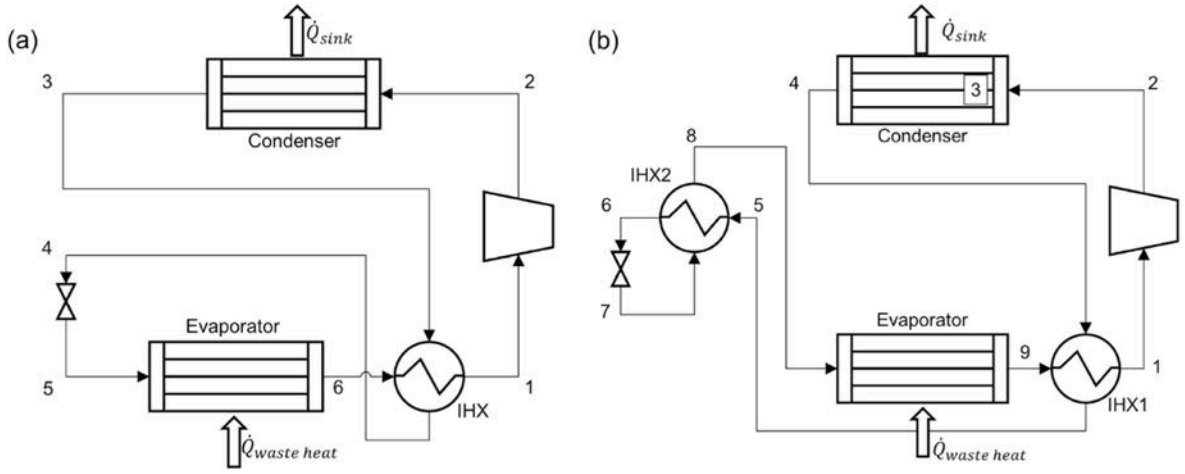

Fig. 1. Heat pump layouts: (a) Standard heat pump cycle [10]; (b) Heat pump cycle for CO_2/acetone mixtures. IHX: Internal Heat Exchanger.

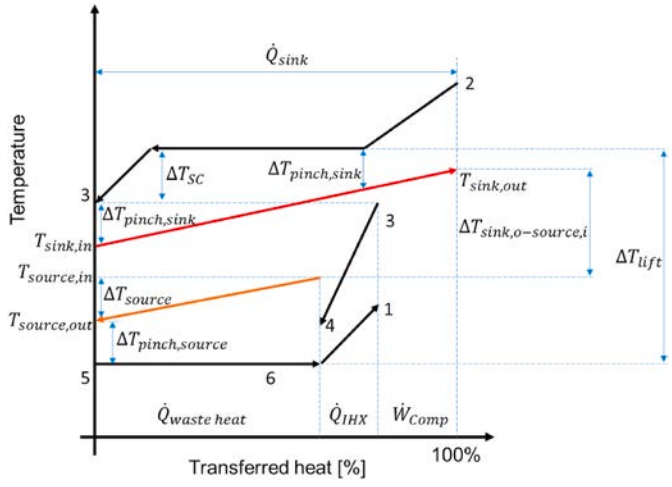

Fig. 2. Temperature-heat diagram for the HTHP shown in Fig. 1-a using pure fluids. Refrigerant in black color. Sink fluid in red color. Source fluid in brown color.

start of the condensation process is identified at state 3. Due to the temperature glide during phase change, saturated vapor (state 3) is identified inside the condenser. The condenser outlet properties (state 4) depend on the CO_2/acetone mixture as there is a high temperature glide between saturated states, which depend on the relative composition of the mixture, as it will be seen in detail in the Results section. Thus, it is necessary to define state 4 as a function of the saturated liquid temperature at high pressure for each CO_2/acetone mixture composition. This ensures that the condenser outlet (state 4) has a larger temperature than the compressor inlet (state 1). Fig. 3 presents the temperature-heat diagram for CO_2/acetone mixtures and the main assumptions used, which are explained in the next section.

Fig. 4 presents the p-h diagrams of the heat pump described in Fig. 1-b for two different compositions: 5% CO_2 + 95% acetone (Fig. 4-a) and 25% CO_2 + 75% acetone (Fig. 4-b), to illustrate the definition of the condenser outlet. Two cases are considered.

1. $T_{bub}(P_{cond}) \geq T_1$:

In Fig. 3-a and Fig. 4-a, the saturated liquid at high pressure is 162 °C ($T_{bub}(P_{cond})$, red dot in Fig. 4-a), which is higher than the compressor inlet temperature of 142 °C. In this case, there is no temperature cross between the outlet heat sink and the inlet source sink. In this way, it is possible to transfer some heat from the subcooled liquid (state 4) to superheat vapor at state 1. The IHX1 is characterized by the temperature difference ($\Delta T_{IHX,1}$) between the subcooled liquid at high pressure (state 5) and the saturated vapor at low pressure (state 9). To simplify the calculations, the subcooled liquid at high pressure (state 6) is considered to be at the same temperature as the saturated vapor at low pressure (state 9). Then, state 6 is throttled after transferring heat to the low-pressure stream (state 7 → 8) in the IHX2. All these assumptions are mathematically explained in the next section (Table 3).

2. $T_{bub}(P_{cond},) < T_1$:

Fig. 3-b and Fig. 4-b show the case where the condenser outlet (state 4) is assumed to be a vapor-liquid mixture to avoid temperature cross between $T_{sink,o}$ and $T_{source,i}$. This is related to the compressor inlet temperature, as shown in Fig. 4-b, where T_4 = 124 °C, while T_1 = 119 °C. The condenser outlet state 4 is calculated from an energy balance in the

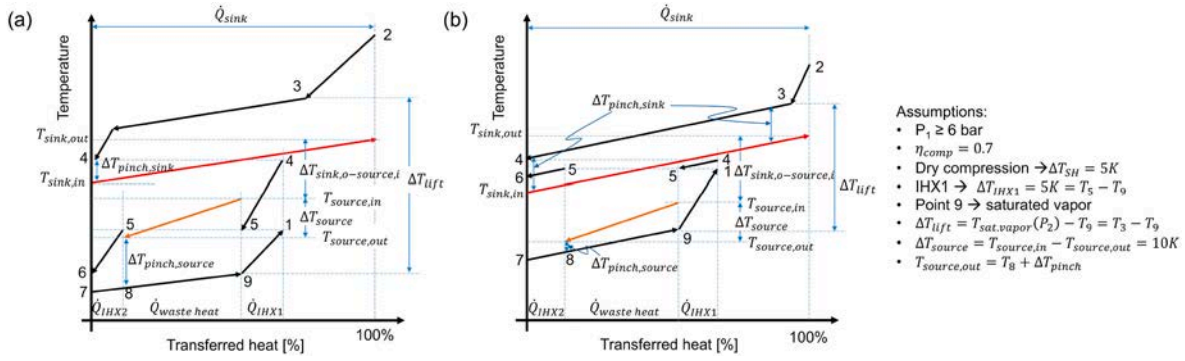

Fig. 3. Temperature-heat diagram and main assumptions for the HTHP shown in Fig. 1-b using CO_2/acetone mixture, (a) case 1 and (b) case 2.

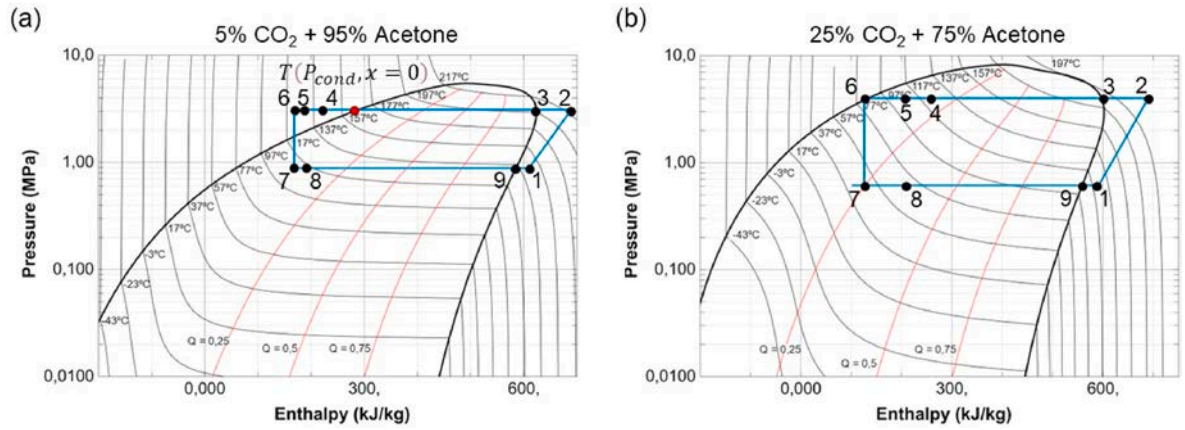

Fig. 4. Pressure-enthalpy diagrams for: (a) 5% CO_2 + 95% acetone and (b) 25% CO_2 + 75% acetone.

IHX1. IHX1 is characterized by $\Delta T_{IHX,1}$ in the same way as in the previous case. The throttle valve inlet (state 6) is considered as saturated liquid at high pressure. Similarly, these assumptions are mathematically explained in the next section (Table 3).

Finally, state 8 is obtained from an energy balance in the IHX2 in both cases. Then, waste heat is used as heat source to complete the evaporation process at the evaporator outlet (state 9).

2.3. Thermodynamic analysis

The heat pump analysis is performed assuming steady state and adiabatic components. The calculations are performed by using a combination of Refprop and Matlab software. Refprop software [45] is employed to obtain the thermodynamic properties of both pure fluids and CO_2/acetone mixture. Table 2 shows the common modelling assumptions used to model both heat pumps shown in Fig. 1.

Fig. 5 summarizes the procedure to calculate the HTHP performance for each refrigerant. Two input parameters are used to calculate the thermodynamic properties for both pure and CO_2/acetone fluids in the HTHP: the temperature lift (ΔT_{lift}) and the temperature difference between the sink outlet temperature and the inlet source temperature ($\Delta T_{sink,o-source,i}$). These parameters and the main assumptions used to calculate the thermodynamic properties of each HTHP are presented in Fig. 2 for pure fluids, and in Fig. 3 for CO_2/acetone mixture. These figures show the $T-\dot{Q}$ diagram for the refrigerants considered pointing out the temperature lift, the temperature difference between the sink outlet and the source inlet, the pinch-point temperature difference in the condenser, and the temperature profile of the heat source (i.e. the

Table 2
Common modelling assumptions for the heat pump designs of the standard cycle (Fig. 1-a) and the heat pump for CO_2/acetone mixture (Fig. 1-b).

Input parameters	Value
Temperature lift (ΔT_{lift})	40, 70, 100 K
Temperature difference between the sink outlet and the source inlet ($\Delta T_{sink,o-source,i}$)	70, 100 K
Compressor' isentropic efficiency (η_{comp})	70%
Mass flow rate of refrigerant ($\dot{m}_{HTF}$)	1 kg/s
Pressure drop in all heat exchangers (ΔP)	0 bar
Heat losses in all devices ($\dot{Q}_{loss}$)	0 W
Temperature difference at the IHX1 ($\Delta T_{IHX,1}$)	5 K
Superheat at the compressor inlet (ΔT_{SH})	5 K
Sink pinch point temperature ($\Delta T_{pinch,sink}$)	2.5 K
Source pinch point temperature ($\Delta T_{pinch,source}$)	2.5 K
Source temperature difference (ΔT_{source})	10 K

Table 3
Equations used to model the heat pump design for CO_2/acetone mixture.

Input parameters		Eq
Pressures	$P_{cond} = p_{sat}(T_3, x=1) < P_{crit}$	(4)
	$P_{evap} = p_{sat}(T_9, x=1) > 6\ bar$	(5)
State point 1	$h_1 = h(P_{evap}, T_{dew}(P_{evap}) + \Delta T_{SH})$	(6)
	$s_1 = s(P_{evap}, h_1)$	(7)
State point 2	$h_{2s} = h(P_{cond}, s_1)$	(8)
	$h_2 = h_1 + (h_{2s} - h_1)/\eta_{comp}$	(9)
State point 3	$h_3 = h_{sat}(P_{cond}, x=1)$	(10)
State point 4	$h_4 = h_5 + h_1 - h_9$	(11)
State point 5	$h_5 = h(P_{cond}, T_9 + \Delta T_{IHX1})$	(12)
State point 6	1. If $T_{bub}(P_{cond}) \geq T_1$: $h_6 = h(P_{cond}, T_9)$	(13)
	2. If $T_{bub}(P_{cond}) < T_1$: $h_6 = h_{sat}(P_{cond}, x=0)$	(14)
State point 7	$h_6 = h_7$	(15)
State point 8	$h_8 = h_5$	(16)
State point 9	$h_9 = h_{sat}(P_{evap}, x=1)$	(17)

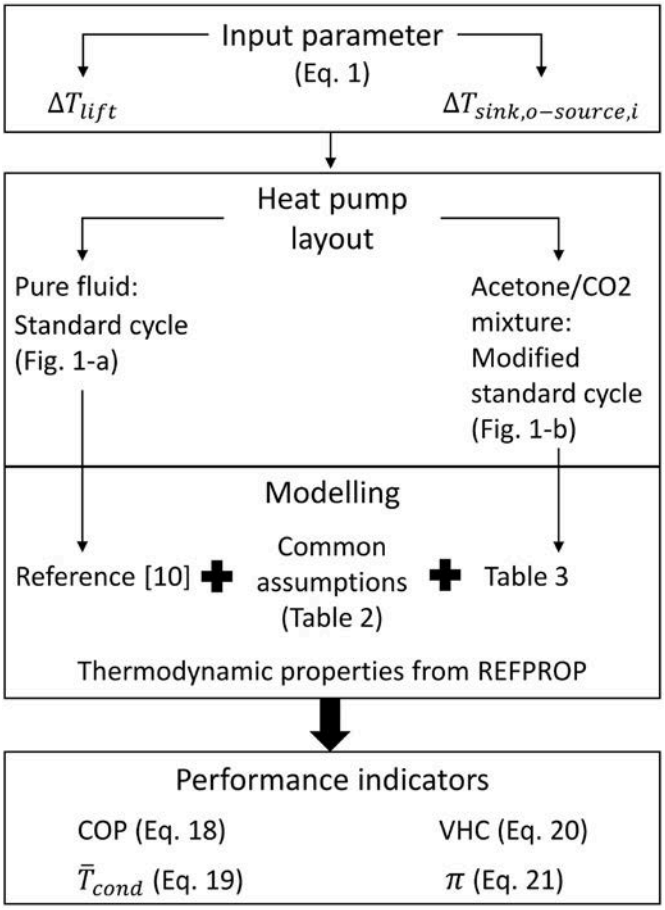

Fig. 5. Schematic of the mathematical model.

recovered waste heat).

To simplify the analysis, air at ambient pressure is used as sink and source fluids. The values of the pinch-point temperature differences in both the evaporator and condenser are close to the values used in Refs. [35,51]. The temperature difference at the source is similar to the value used in Refs. [20,35]. Mass flow rates of air as sink and source are calculated considering the pinch point values shown in Table 2 and performing energy balances in the condenser and the evaporator. The definition of both sink and source pinch points is shown in Fig. 2 for pure fluids and in Fig. 3 for the proposed CO_2/acetone mixture.

The first input parameter is the temperature lift, which is straightforward to calculate for pure fluids with constant phase change temperature as it is calculated between saturated states at high and low pressure [10], Eq. (1). This parameter gives information about the maximum and minimum temperatures of the heat sink and the heat source, respectively. The temperature lift used when working with the CO_2/acetone mixture is also defined by Eq. (1).

$$\Delta T_{lift} = T_{dew}(P_{cond}) - T_{dew}(P_{evap}) \tag{1}$$

When working with zeotropic mixtures, this temperature lift gives information about the saturated vapor at high pressure in the condenser inlet (state 3, Fig. 3) and the saturated vapor at low pressure in the evaporator outlet (state 9, Fig. 3). Both states 3 and 9 are selected to define ΔT_{lift} due to their relationship with the sink and source temperatures. State 3 determines the discharge sink temperature ($T_{sink,o}$) by the pinch-point temperature ($\Delta T_{pinch,sink}$), while state 9 determines the inlet source temperature, which is the inlet temperature of the waste heat, as depicted in Fig. 3.

The second input parameter employed to solve the HTHP cycle is the temperature difference between the sink outlet temperature and the inlet source temperature, Eq. (2). This parameter is calculated as a function of the pinch-point temperature difference in both the condenser and the evaporator and the temperature difference between the source streams. It provides information about the available temperatures obtained in the sink and source fluid (i.e. air) for an application case.

$$\Delta T_{sink,o-source,i} = T_{sink,o} - T_{source,i} \tag{2}$$

The basic equations and assumptions used to model the standard cycle for pure fluids (Fig. 1-a, and Fig. 2) are detailed in Ref. [10].

The equations and assumptions to model the heat pump for the CO_2/acetone mixture (Fig. 1-b and Fig. 3) are presented in Table 3. Note that the minimum evaporator pressure is limited to 6 bar to avoid the likely phase transition of CO_2 from gas to solid, although lower pressures might be feasible according to the vapor-liquid equilibrium data reported in Refs. [33,52]. Therefore, the saturated vapor state at low pressure is within the limits shown in Eq. (3), which range from 6 bar to the critical temperature of the mixture. The hot sink temperature is also limited to be 25 K below the critical temperature of each refrigerant to avoid working near critical conditions:

$$T_9 \in \left[T_{dew}(P = 6\ bar), T_{crit} - 25K - \Delta T_{lift}\right] \tag{3}$$

It is worth noting that no limitation is imposed on the temperature at the compressor outlet. Several works limit this temperature up to 180 °C to avoid the thermal decomposition of the compressor lubricant [20,37]. However, there are available oil-free technologies that may overcome this limitation [39].

No heat transfer analysis has been performed to size the heat exchangers area, and thus, to estimate the costs of the heat pump. Such analysis should consider that the phase-change of a zeotropic fluid is a non-equilibrium process, since during condensation, the less volatile component is prone to condense at dew point, while the more volatile component of the mixture is accumulated at the interface of the liquid condensate and vapor [29]. Therefore, specific mass transfer and heat mass transfer resistances should be accounted to size the heat exchangers [22,53,54]. Future works should model and validate experimentally the mass and heat transfer coefficients of the proposed mixture during condensation.

2.4. Performance indicators

The thermodynamic performance for both configurations is measured by the coefficient of performance (COP), which is the ratio of useful heating transferred to the heat sink in the condenser to the work performed by the compressor:

$$COP = \frac{\dot{Q}_{sink}}{\dot{W}_{comp}} \tag{18}$$

The COP is a straightforward performance indicator to compare between fluids that show a constant temperature during phase change. However, difficulties appear to compare COP results of pure fluids and zeotropic mixtures. Therefore [51,55], employed the Lorenz efficiency [56] to account for the temperature glides $COP_{Lor} = \overline{T}_{sink}/(\overline{T}_{sink} - \overline{T}_{source})$, where $\overline{T}_{sink}$ and $\overline{T}_{source}$ are the thermodynamic average temperatures defined as $\overline{T} = \Delta h/\Delta s$.

In this work, however, the COP definition (Eq. (18)) is preferred as it is a direct indicator of the heat rejected in the condenser. Thus, the classic COP definition is calculated (Eq. (18)). Similarly to Ref. [51], the thermodynamic average temperature in the condenser is used to consider the temperature glide, and thus, to be able to compare between pure and zeotropic fluids:

$$\overline{T}_{cond} = \frac{\Delta h}{\Delta s} = \frac{h_2 - h_4}{s_2 - s_4} \tag{19}$$

For pure fluids, Eq. (19) is close to the saturation temperature at high pressure due to the constant temperature during phase change and the

high enthalpy of vaporization. For the CO_2/acetone mixture, the thermodynamic average temperature in the condenser is affected by the temperature glide of the mixture.

Other yield indicators used are the volumetric heating capacity, the pressure ratio and the outlet temperature of the heat sink. The volumetric heating capacity (VHC) evaluates the heat supplied in the condenser per unit of compressed volume flow rate of refrigerant. This gives information about the compressor size, meaning that high VHC are related to small compressors and low compressor capital cost [20].

$$VHC = (h_2 - h_4)\cdot\rho_1 \tag{20}$$

The pressure ratio (π) is defined as the relation between high and low pressures, which are calculated for each case as a function of the condenser temperature and the temperature lift, as shown in Table 3. Lower pressure ratios are likely to result in larger compressor efficiencies.

$$\pi = \frac{P_{cond}}{P_{evap}} \tag{21}$$

The outlet temperature of the heat sink ($T_{sink,o}$) is calculated performing an energy balance on the condenser knowing the pinch point temperature difference ($\Delta T_{pinch,sink}$), as shown in Table 1 and Fig. 3. Air at ambient pressure is modelled as the sink fluid. A mass flow of $\dot{m}_{HTF} = 1\ kg/s$ of refrigerant is considered for each HTHP case.

3. Results and discussions

This section analyzes the behavior of the proposed mixture working in a heat pump for high temperature applications. First, the effect of the CO_2/acetone composition on the thermodynamic properties is studied. Then, the HTHP performance indicators are presented as a function of the input parameters (ΔT_{lift} and $\Delta T_{sink,o-source,i}$) to compare between pure fluids and CO_2/acetone mixture. In the first case, $\Delta T_{lift} = 40, 70, 100\ K$ are considered to calculate all the thermodynamic properties of the cycle. In the second case, $\Delta T_{sink,o-source,i} = 40, 70, 100\ K$ are considered to evaluate the HTHP behavior assuming air as the sink and source fluid. Note that when $\Delta T_{sink,o-source,i}$ is fixed, ΔT_{lift} varies, and vice versa, due to their definition (Eqs. (1) and (2)). Note that the CO_2 and acetone contents in each mixture is expressed as mass fractions.

3.1. Effect of the mixture composition on thermodynamic properties

Fig. 6 compares the critical pressure and temperature calculated using Refprop [45] with experimental data [57–59], estimated data using Peng-Robinson equation of state [58], and simulated data from literature [60]. The reported experimental data is focused on low mass fractions of acetone. In this range, Refprop results show a good agreement with the experimental results. Peng-Robinson modeling results [58] are also included. When increasing the acetone mass fraction in the binary mixture, only the molecular modeling performed in Ref. [60] extends the thermodynamic conditions to compare with Refprop results. Acetone mass fractions from 10% to 30% are between the molecular simulations of [60] and the Peng-Robinson modeling of [58]. Refprop results for larger acetone mass fractions show similar trend to Ref. [60], obtaining a close prediction of the critical conditions for pure acetone [59].

The phase envelopes of pure CO_2, pure acetone and the proposed binary mixtures are compared in Fig. 7. High temperature glides are shown for the CO_2/acetone mixtures. The increase of the CO_2 mass fraction reduces the critical temperature of the mixture, and thus, its possible utilization for high temperature applications. As the proposed HTHPs (Fig. 1) work under subcritical conditions for condensing temperatures above 100 °C, the mixtures with a mass fraction of CO_2 greater than 50% are disregarded. Only the mixtures with low content of CO_2 are likely to meet the target high temperatures. Regarding the pressure, the condenser should work at a pressure range of about 25–35 bar to achieve dew point temperatures greater than 150 °C.

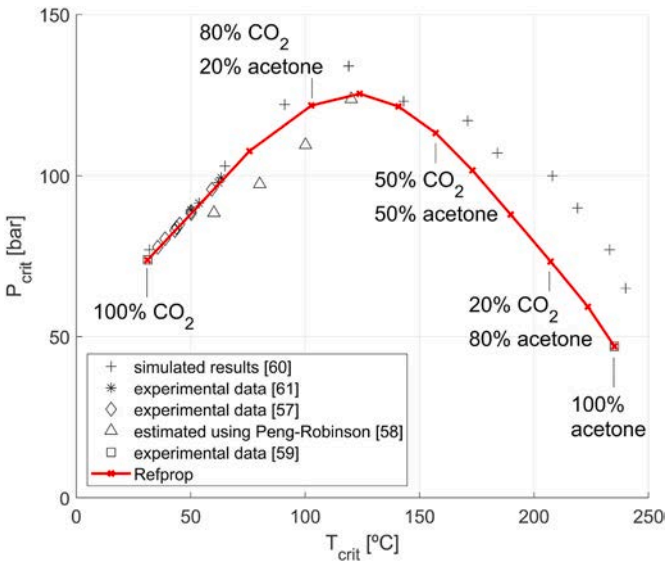

Fig. 6. Critical temperature and pressure as a function of the CO_2/acetone mixture composition. Binary mixture results are calculated in steps of 10% in mass fraction. The red lines connecting the points are guides to the eye. [61].

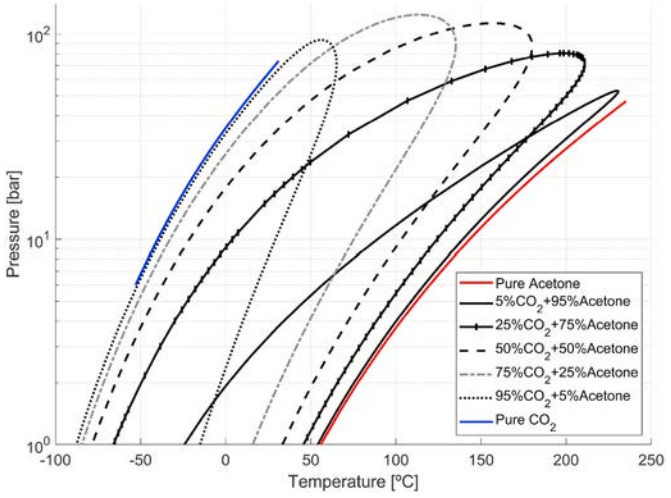

Fig. 7. Phase envelope for pure acetone, CO_2/acetone mixtures in mass fraction and pure CO_2.

The phase envelopes (Fig. 7) as well as the temperature glide values (Fig. 8) are useful to understand the effect of mixture composition changes due to refrigerant leakages during the HTHP operation. The high temperature glide introduced in Fig. 7 can be seen in detail in Fig. 8, where the temperature glide is plotted for several pressures as a function of the CO_2 mass fraction in the mixture. The temperature glide changes with the mixture composition and the pressure. Regarding the composition, the higher the CO_2 mass fraction in the binary mixture, the higher the temperature glide up to a mass fraction of 22% CO_2, which is in accordance with [28]. Regarding the pressure, overall, the higher the pressure (i.e. the condensing temperature), the lower the temperature glide, as shown in Ref. [29]. This trend changes for CO_2 contents between 22% and 75%.

The temperature glide is usually limited to about 50 K to avoid a high condensation shift and the fractionation of the components in the condenser [23,40]. Such temperature glides are obtained for mixtures with 10% or 95% of CO_2 at 40 bar (Fig. 8). However, the pressure also

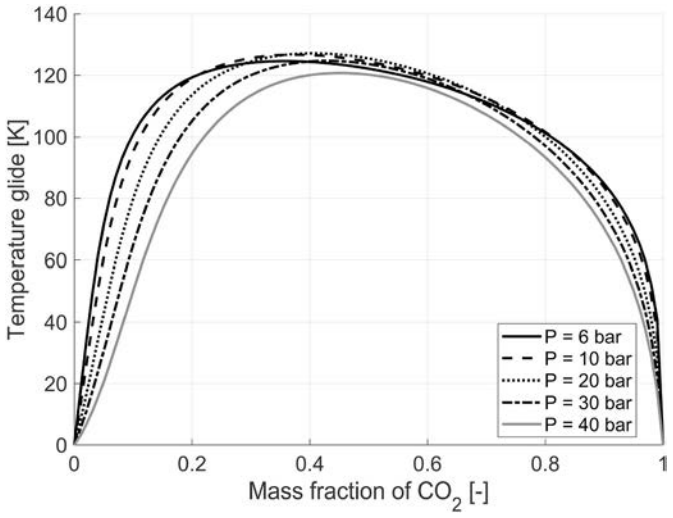

Fig. 8. Variation of the temperature glide with the CO2/acetone mixture composition for several pressures.

plays a significant role. For instance, the 5% CO_2/95% acetone mixture shows a temperature glide of 61 °C at 10 bar, and a temperature glide of 43 k at 20 bar, which are around the current temperature glide limitation. Therefore, the most promising CO_2/acetone mixtures range between 5% CO_2 and 10% CO_2, which agrees with the critical temperatures shown in Fig. 5. Nevertheless, the next sections further study the CO_2/acetone mixtures with CO_2 contents up to 50% in mass fraction to fully analyze the mixture performance.

3.2. Performance results as function of ΔT_{lift}

Fig. 9 shows the performance indicators of HTHPs for pure fluids and different CO_2/acetone compositions. COP (Fig. 9-a), VHC (Fig. 9-b), pressure ratio (Fig. 9-c) and compressor outlet temperature (Fig. 9-d) are plotted as a function of the average thermodynamic temperature in the condenser (Eq. (19)) for a temperature lift of $\Delta T_{lift} = 40\ K$. The results for the standard cycle working with pure refrigerants have been validated with the results reported in Ref. [10].

An optimum COP is obtained as $\overline{T}_{cond}$ increases for each refrigerant (Fig. 9-a). For pure fluids, the condensation temperature that maximizes the COP is approximately 20–60 K below the critical point of each fluid, in agreement with [35,62]. This result is explained by the narrowing of the two-phase region as the condensation temperature increases [10]. The same trend is observed for 5% CO_2/95% acetone and 10% CO_2/90% acetone mixtures. Such an optimum is not shown for mixtures containing 25% and 50% of CO_2, which may be due to the evaporator pressure limitation ($P_1 \geq 6\ bar$) that reduces the condensation temperature range. It is worth noting that there is a significant COP reduction when increasing the CO_2 in the mixture. This tendency is explained by the change in the p-h diagram as a function of the mixture composition. As the mass fraction of CO_2 increases, the condenser outlet (state 4) changes from subcooled liquid to vapor-liquid mixture as the condenser outlet is kept at a higher temperature than the compressor inlet (state 1). This is produced by the high temperature glide, reducing the heat rejected in the condenser, and thus, decreasing the COP.

The 5% CO_2/95% acetone mixture shows the maximum $COP_{max} = 7.87$ at $\overline{T}_{cond} = 184.8^{o}C$ compared to the rest of refrigerants. Higher CO_2 mass fractions reduce the COP. Indeed, the 10% CO_2/90% acetone mixture shows lower performance than pure acetone. Two effects may explain such a behavior. On the one hand, the increase of the CO_2 mass

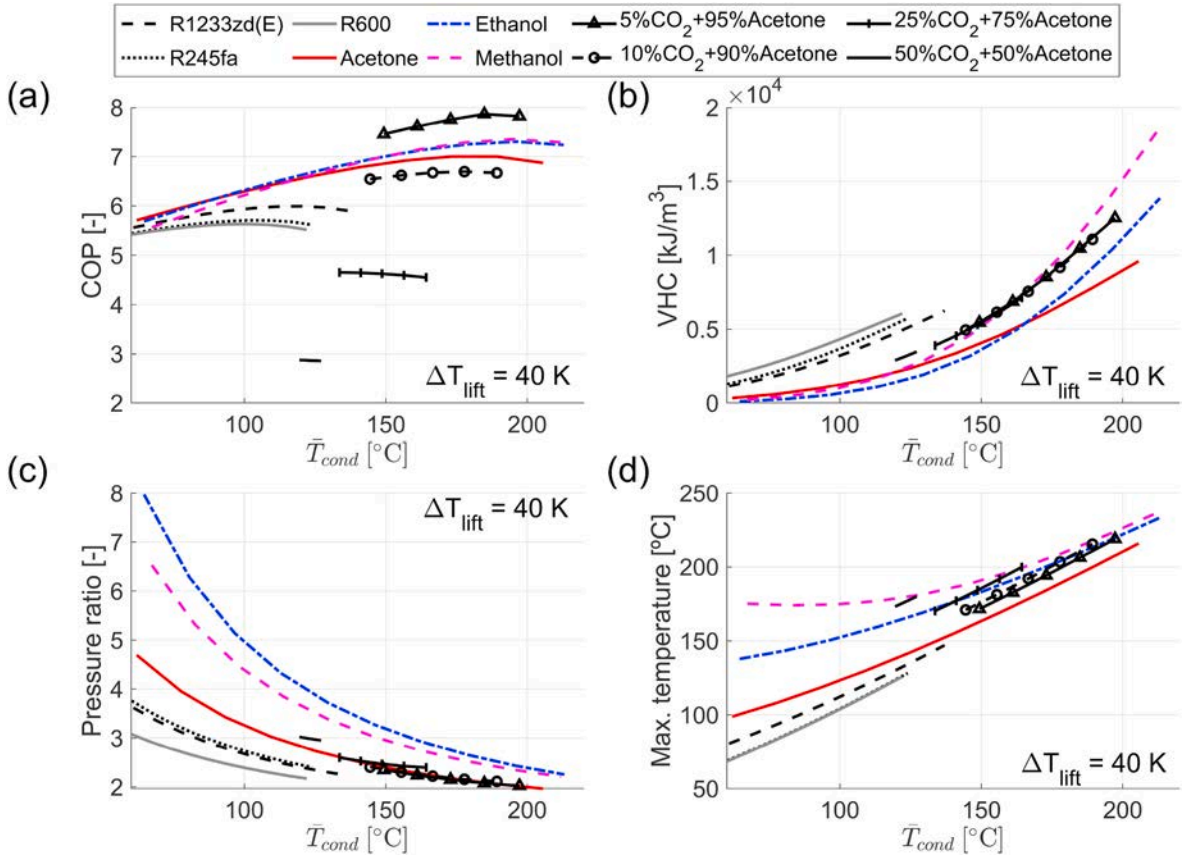

Fig. 9. HTHP behavior for a temperature lift of $\Delta T_{lift} = 40$ K as a function of the thermodynamic average temperature in the condenser ($\overline{T}_{cond}$): (a) COP, (b) VHC, (c) pressure ratio and (d) maximum discharge temperature.

fraction, increases the mixture enthalpy. On the other hand, the larger the CO_2 contained in the mixture, the less the enthalpy change between dew and bubble points at high pressure, as shown in Fig. 4. This means that the enthalpy change at the condenser is reduced when a rich CO_2 mixture is employed.

Regarding the pure refrigerants, close COP values to 5% CO_2/95% acetone mixture are obtained for methanol ($COP_{max} = 7.35$ and $\overline{T}_{cond} = 195^oC$) and ethanol ($COP_{max} = 7.3$ and $\overline{T}_{cond} = 196^oC$). Pure acetone shows lower performance ($COP_{max} = 7.0$ and $\overline{T}_{cond} = 182.5^oC$) than the 5% CO_2/95% acetone mixture. Thermodynamic properties (temperature, pressure, enthalpy and entropy) of pure fluids (acetone, ethanol and methanol) and CO_2/acetone mixtures (5% CO_2/95% acetone and 10% CO_2/90% acetone) are included as Supplementary material for $\Delta T_{lift} = 70\ K$ and $\overline{T}_{cond} = 175^oC$, which are plotted in Fig. 10-a. Mass flow rates and temperatures of air working as heat sink and heat source are also presented in such tables.

As reported in Ref. [10], VHC values for reciprocating piston and screw compressors are recommended to be in the range of 3000 kJ/m^3 to 6000 kJ/m^3, showing a lower practical limit of 1000 kJ/m^3. Centrifugal compressors are also considered in Ref. [20]. The VHC of the studied refrigerants is presented in Fig. 9-b for $\Delta T_{lift} = 40\ K$. The values of all the refrigerants considered are above the lowest practical limit. Furthermore, the proposed mixture improves the VHC results compared to pure acetone.

Fig. 9-c compares the pressure ratio of the pure refrigerants and the proposed mixture. The pressure ratio decreases with higher average condensation temperatures due to the increase of the evaporation pressure [10]. The CO_2/acetone mixtures obtain pressure ratios in the range of 2–3 for condensing temperatures of 120–200 °C, in a similar way as pure acetone.

The maximum temperature in the cycle is obtained at the compressor outlet (Fig. 9-d). As mentioned above, low discharge temperatures are preferred to reduce the likely thermal decomposition of lubricant in the compressor technologies that require lubrication [20]. However, oil-free centrifugal compressors could overcome this issue [39]. The proposed mixture slightly increases the discharge temperature compared to pure acetone. A difference of 10 K is shown for 5% CO_2/95% acetone mixture compared to pure acetone. Discharge temperature increases with the mass fraction of CO_2, reaching the maximum temperatures of pure methanol in some cases.

Fig. 10 compares the HTHP behavior for pure refrigerants and the proposed mixture considering a temperature lift of 70 *K*. In this case, the mixture compositions are limited to CO_2 mass fractions that range from 5% to 25%. As aforementioned, the larger ΔT_{lift}, the lower the application range due to the evaporator pressure limitation (Eq. 5, Table 3) and the decrease of the critical temperature (Fig. 6).

The mixtures with 5% and 10% mass fractions of CO_2 show better COP (Fig. 10-a) and VHC (Fig. 10-b) than pure refrigerants. The CO_2 effect on the mixture behavior is remarkably high when comparing with pure acetone. In this regard, although the mixture composition with 25% of CO_2 shows a slightly lower COP than pure acetone, it also shows an increase in VHC.

The pressure ratios obtained with the CO_2/acetone mixtures are similar to pure acetone (Fig. 10-c). The maximum cycle temperature for the 5% CO_2/95% acetone mixture is 10 K above pure acetone (Fig. 10-d), following the same behavior as in Fig. 9-d. In the same way, methanol shows the highest discharge temperatures of all fluids considered.

Finally, COP versus the outlet temperature of the air working as the heat sink fluid is plotted in Fig. 11 for different temperature lifts. It can be seen that the mixture with a CO_2 mass fraction of 5% shows the highest COP for all the temperature lifts studied. In the same way, the COP difference between this mixture and the best pure fluid, methanol, increases from about 0.5 for $\Delta T_{lift} = 40\ K$ (Fig. 11-a) to 1.2 for $\Delta T_{lift} =$

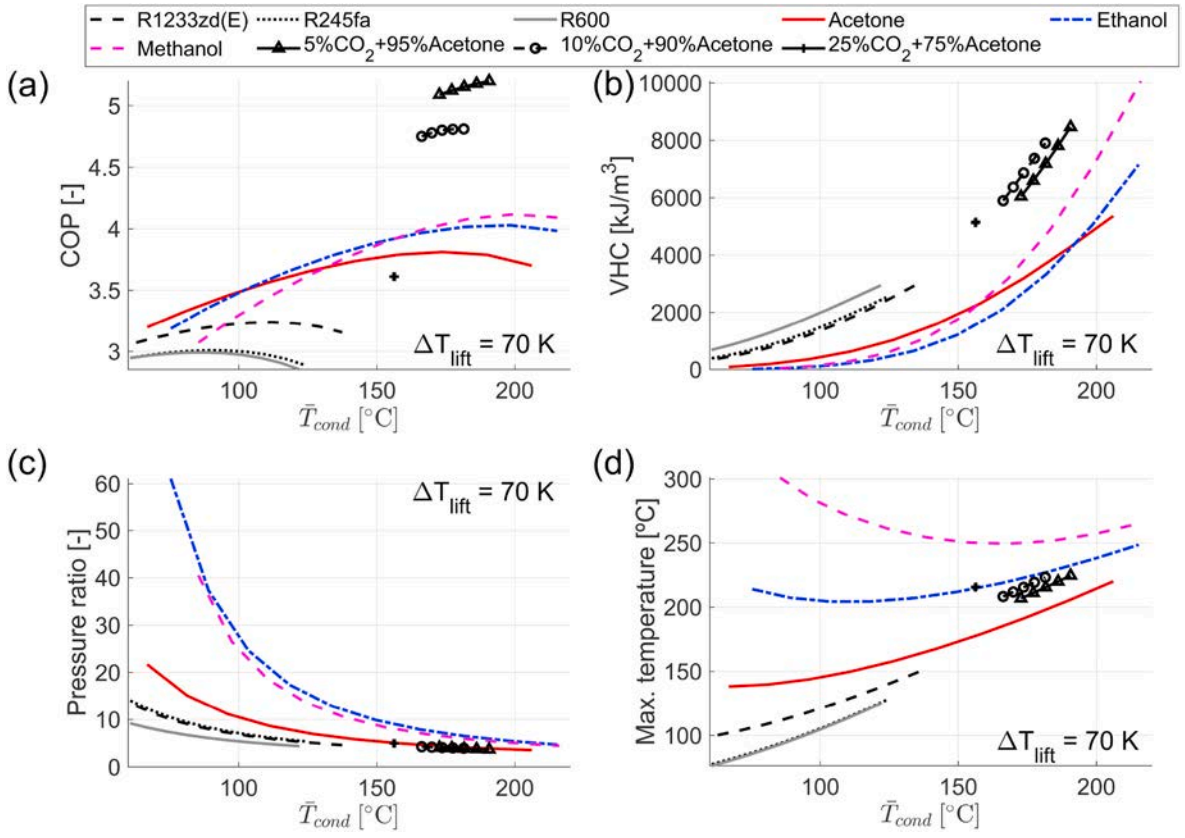

Fig. 10. HTHP behavior for a temperature lift of $\Delta T_{lift} = 70\ K$ as a function of the thermodynamic average temperature in the condenser ($\overline{T}_{cond}$): (a) COP, (b) VHC, (c) pressure ratio and (d) maximum discharge temperature.

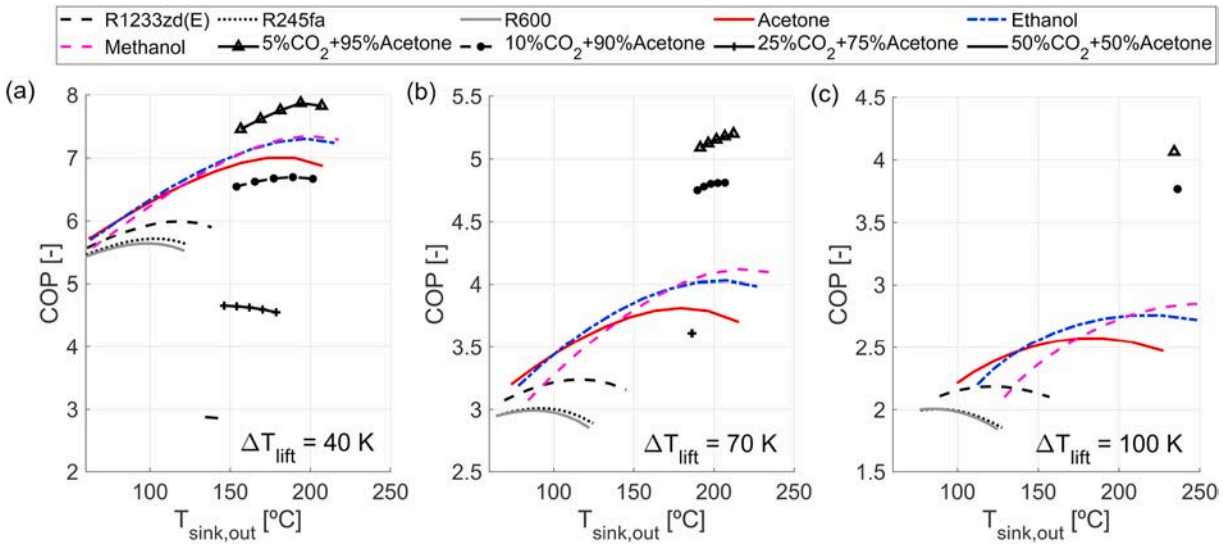

Fig. 11. Outlet temperature of the heat sink for different temperature lifts for different fluids: (a) $\Delta T_{lift} = 40\ K$, (b) $\Delta T_{lift} = 70\ K$ and (c) $\Delta T_{lift} = 100\ K$.

100 K (Fig. 11-c). Therefore, the new proposed mixture shows good performance for large temperature lifts.

3.3. Performance results as function of $\Delta T_{sink,o-source,i}$

This section compares the behavior of pure fluids and the proposed mixture fixing the temperature difference between the outlet heat sink and the inlet heat source to $\Delta T_{sink,o-source,i} = 40\ K, 70\ K$ and 100 K. Therefore, as the input parameter is $\Delta T_{sink,o-source,i}$, the temperature lift varies for each simulation case.

Fig. 12-a shows that, for a temperature difference of 70 K between the outlet heat sink and the inlet heat source, both compositions with a mass fraction of 5% CO_2 and 10% CO_2 present similar COP values, which are larger than pure refrigerants. The better performance of the proposed mixture can be explained by the effect of the temperature glide. For a given $\Delta T_{sink,o-source,i}$, the binary CO_2/acetone mixtures show lower ΔT_{lift} than pure refrigerants when there is a large temperature difference between the inlet and the outlet of the condenser. This is due to the

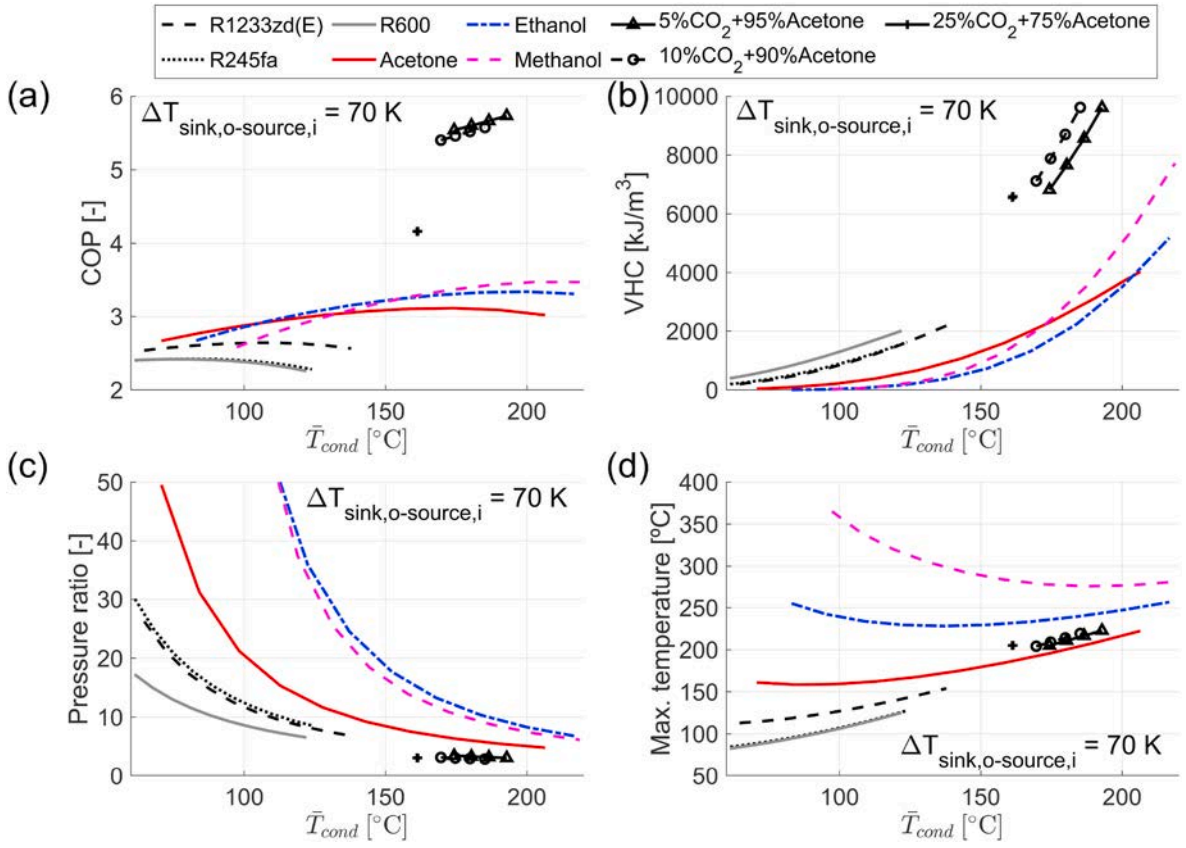

Fig. 12. Performance indicators for the HTHP working with pure fluids and different compositions of CO_2/acetone at $\Delta T_{sink,o-source,i} = 70\ K$: (a) COP, (b) VHC, (c) pressure ratio, and (d) maximum discharge temperature.

gliding effect of the heat sink fluid for the binary mixture. The same applies for the evaporator improving the HTHP performance. This is in accordance with previous works analyzing zeotropic fluids [22,51]. However, when pure refrigerants are analyzed, ΔT_{lift} increases to obtain the same $\Delta T_{sink,o-source,i}$ due to the constant temperature during phase change (Fig. 2). It can be noticed that, when heat sink and source have constant temperatures, the benefit shown by the temperature glide might be lost.

Fig. 12-b shows larger VHC values for the proposed mixture than pure refrigerants. In the same way, CO_2/acetone mixture has the lowest pressure ratio at high condensing temperatures (Fig. 12-c). The CO_2/acetone mixture analyzed show maximum temperatures about 10 K above pure acetone, in a similar way as shown in previous sections.

Fig. 13 summarizes the effect of mixing CO_2 with acetone for different $\Delta T_{sink,o-source,i}$ as a function of the sink outlet temperature. It can be seen that the 5% CO_2/95% acetone mixture has the best performance for all cases. However, similar results can be obtained for the 10% CO_2/90% acetone mixture with large $\Delta T_{sink,o-source,i}$ values. This is because of the ΔT_{lift} values needed to meet $\Delta T_{sink,o-source,i} = 70\ K$ (Fig. 13-b) and 100 K (Fig. 13-c), which reduce the COP values of the 5% CO_2/95% acetone mixture.

Outlet sink temperatures of 200 °C are needed in several industrial processes, such as paper drying, chemical distillation, food drying, plastic injection and metal drying [10]. A HTHP application example working at $T_{sink,o} = 200^oC$ is presented in Table 4 comparing pure acetone and the 5% CO_2/95% acetone mixture. The simulation results presented in Table 4 are shown in Fig. 13-b for $\Delta T_{sink,o-source,i} = 70\ K$. Besides, note that these results are obtained following the assumptions explained in previous sections (Table 3), which consider common thermodynamic constraints for HTHP [10,20].

Although this work is focused on the thermodynamic analysis of the new mixture, it is worth to consider the initial design of the compressor. In this sense [63,64], describe design methodologies for gas lubricated turbo compressors for vapor compression heat pumps. Following these methodologies and applying them to the operating conditions described in Table 4, it was determined that a compressor rotor with a diameter of 0.09 m, rotating at approximately 66,000 RPM could achieve the desired pressures and temperatures. Key challenges in this design would be realizing the small clearance of approximately 60 μm between the compressor rotor and casing. This clearance is required to achieve a compressor efficiency in the range of 80–85%. A larger clearance would reduce the compressor efficiency.

Table 4
Main HTHPs results for pure acetone and 5% CO_2/95% acetone mixture for $\Delta T_{sink,o-source,i} = 70\ K$ and $T_{sink,o} = 200^oC$.

Component	Property	Pure acetone	5% CO_2/95% acetone mixture
Compressor	Inlet temperature [°C]	123.3	138.6
	Outlet temperature [°C]	219.8	213.7
	Mass flow of refrigerant [kg/s]	1	1
Condenser	Pressure [bar]	28.5	28.6
	Outlet temperature [°C]	197.2	142.5
Heat sink	Inlet temperature [°C]	194	140
	Outlet temperature [°C]	200	200
	Air mass flow [kg/s]	52.3	7.4
Heat source	Inlet temperature [°C]	130	130
	Outlet temperature [°C]	120	120
	Air mass flow [kg/s]	21.3	37.1
Evaporator	Pressure [bar]	5.8	8.8
	Inlet temperature [°C]	118.3	117.8
	Outlet temperature [°C]	118.3	133.6
HTHP	COP [−]	3.03	5.63

Overall, the 5% CO_2/95% acetone mixture presents better performance than pure acetone, even showing similar outlet compressor temperatures. A drawback of the proposed mixture might be the temperature glide of 53.3 K in the condenser, which is near the accepted constraint of 50 K. However, its high COP justifies the thermodynamic study performed in this work, and encourages the future design of heat exchangers to ensure a good mixing during the zeotropic condensation, and thus, to obtain a reduced heat exchanger area.

4. Conclusions

This paper addresses the thermodynamic analysis of CO_2/acetone mixtures, which show zeotropic behavior, working as the refrigerant of high temperature heat pumps for temperatures higher than 150 °C. The thermodynamic characterization of the CO_2/acetone mixtures shows temperature glides below 50 K for CO_2 mass fractions up to 10%. Higher CO_2 concentrations in the binary mixture produce large temperature glides in the range of 50–120 K. Therefore, any leakage that can change the mixture composition should be prevented in order to ensure the proper zeotropic condensation process.

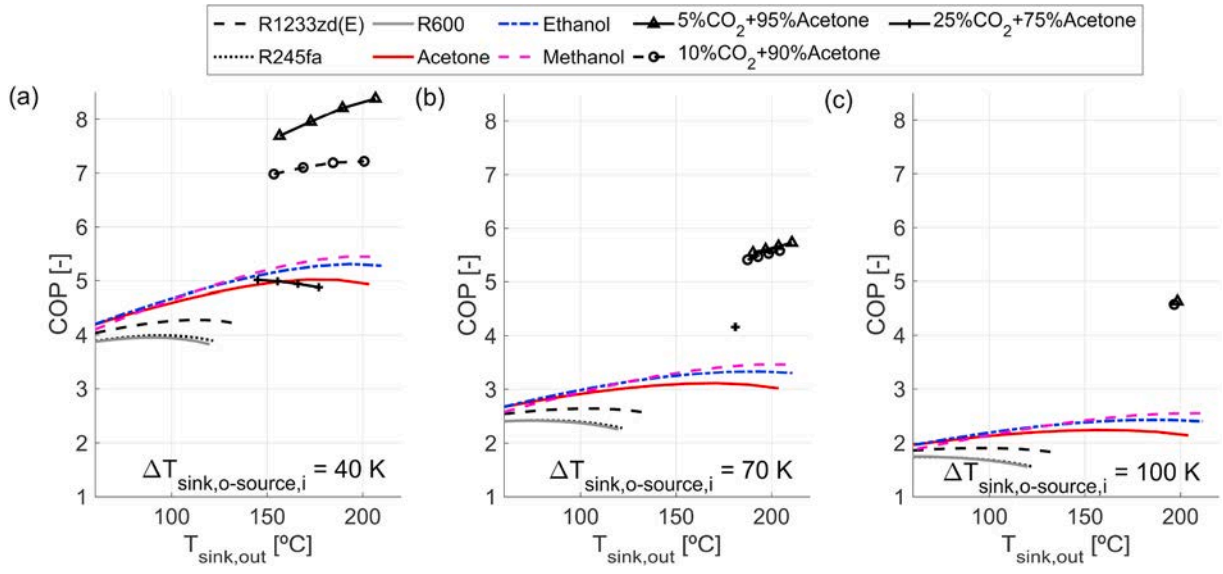

Fig. 13. Outlet temperature of the heat sink for different $\Delta T_{sink,o-source,i}$ and for different fluids: (a) $\Delta T_{sink,o-source,i} = 40\ K$, (b) $\Delta T_{sink,o-source,i} = 70\ K$ and (c) $\Delta T_{sink,o-source,i} = 100\ K$.

The new fluid is compared with existing pure refrigerants currently used in high temperature applications. The HTHP configuration for pure refrigerants assumes a simplified heat pump cycle equipped with an internal heat exchanger. Similar conditions and HTHP configuration are modelled to study the binary mixture. The main difference is the use of a second internal heat exchanger to ensure the complete condensation of the zeotropic mixture. The HTHP performance results are presented assuming that waste heat from an industrial process is the heat source. Air is considered as both the heat sink and heat source. Two input parameters are used to study the HTHP performance: the temperature lift between the condenser inlet and the evaporator outlet, and the temperature difference between the outlet heat sink and the inlet heat source are studied.

When the temperature lift is used as input parameter, the mixture composed by 5% CO_2 and 95% acetone in mass fraction shows the best performance compared to pure fluids in all cases. For such a mixture, the higher the temperature lift, the higher the difference compared to pure acetone. The 5% CO_2/95% acetone mixture can reach outlet sink temperatures of 200 °C for $\Delta T_{lift} = 70\ K$ with a performance of $COP = 5.15$, which is an improvement of 26% compared to pure acetone. Concentrations up to 10% CO_2 in mass fraction also show performance improvements for high temperature lifts, while this mixture gives COP values 4% less than pure acetone for low temperature lifts ($\Delta T_{lift} = 40\ K$).

When the temperature difference between the outlet heat sink and the inlet heat source is used as input parameter, the mixture composed by 5% CO_2 and 95% acetone in mass fraction also shows the best performance indicators. In this case, the favorable effect of the temperature glide for zeotropic mixtures improves the HTHP performance, and thus, even the 10% CO_2 and 90% acetone mixture in mass fraction presents higher COP values than all pure refrigerants. For instance, the 5% CO_2/95% acetone mixture shows a COP improvement of 46% compared to pure acetone when the target outlet sink temperatures is 200 °C and the temperature difference is $\Delta T_{sink,o-source,i} = 70\ K$, obtaining $COP = 5.63$.

In all cases, the mixture 5% CO_2 and 95% acetone in mass fraction shows that the maximum temperature at the compressor outlet only increases about 10 K compared to pure acetone. Furthermore, the larger the temperature lift, the higher the difference of the maximum temperatures at the compressor outlet between pure methanol and the CO_2/acetone mixture. The mixture 5% CO_2 and 95% acetone in mass fraction shows the highest volumetric heating capacities. Pressures in the range of 25–35 bar are needed in the condenser for this binary mixture, which are slightly higher than for pure acetone.

To conclude, the proposed binary mixture of CO_2 and acetone shows significative performance improvements compared to pure refrigerants for a single-stage HTHP configuration with internal heat exchanger. The best HTHP performance is shown for the mixture 5% CO_2/95% acetone in mass fraction. The mixture 10% CO_2/90% acetone in mass fraction also presents good performance indicators. Changes in the binary mixture composition, which might be caused due to refrigerant leakages, should be avoided to maintain the temperature glide in values around 50 K. Further works should study the modeling and experimental validation of mass transfer and heat transfer for proposed CO_2/acetone mixture. In the same way, new heat exchanger designs would be needed to improve the phase mixing during the zeotropic condensation, reducing the mass transfer resistances, and therefore, achieve cost-effective heat exchangers.

Credit author statement

Gómez-Hernández, Jesús: Conceptualization, Methodology, Software, Writing. Grimes, Ronan: Conceptualization, Methodology, Writing. Marugán-Cruz, Carolina: Writing – original draft. Briongos, Javier Villa: Supervision, Review and Editing. Santana, Domingo: Supervision.

Declaration of competing interest

The authors declare that they have no known competing financial interests or personal relationships that could have appeared to influence the work reported in this paper.

Data availability

Data will be made available on request.

Acknowledgements

This work has been supported by the Madrid Government (Comunidad de Madrid-Spain) under the Multiannual Agreement with UC3M in the line of Excellence of University Professors (EPUC3M22), and in the context of the V PRICIT (Regional Programme of Research and Technological Innovation).

Appendix A. Supplementary data

Supplementary data to this article can be found online at https://doi.org/10.1016/j.energy.2023.126821.

References

[1] IEA (2022), Heating, IEA, Paris https://www.iea.org/reports/heating, License: CC BY 4.0.
[2] Heat Roadmap Europe. Heating and cooling: facts and figures, the transformation towards a low-carbon heating and cooling sector. 2017.
[3] Thiel GP, Stark AK. To decarbonize industry, we must decarbonize heat. Joule 2021;5:531–50. https://doi.org/10.1016/J.JOULE.2020.12.007.
[4] Olsson O, Schipfer F. Decarbonizing industrial process heat: the role of biomass. 2021.
[5] European Commission. Powering a climate-neutral economy: an EU strategy for energy system integration. 2020.
[6] Papapetrou M, Kosmadakis G, Cipollina A, La Commare U, Micale G. Industrial waste heat: estimation of the technically available resource in the EU per industrial sector, temperature level and country. Appl Therm Eng 2018;138:207–16. https://doi.org/10.1016/j.applthermaleng.2018.04.043.
[7] Men Y, Liu X, Zhang T. A review of boiler waste heat recovery technologies in the medium-low temperature range. Energy 2021;237:121560. https://doi.org/10.1016/J.ENERGY.2021.121560.
[8] Wang Y, Wang J, He W. Development of efficient, flexible and affordable heat pumps for supporting heat and power decarbonisation in the UK and beyond: review and perspectives. Renew Sustain Energy Rev 2022;154:111747. https://doi.org/10.1016/J.RSER.2021.111747.
[9] ITP Thermal Pty Ltd. Renewable energy options for industrial process heat. 2019.
[10] Arpagaus C, Bless F, Uhlmann M, Schiffmann J, Bertsch SS. High temperature heat pumps: market overview, state of the art, research status, refrigerants, and application potentials. Energy 2018;152:985–1010. https://doi.org/10.1016/j.energy.2018.03.166.
[11] Jiang J, Hu B, Wang RZ, Deng N, Cao F, Wang C-C. A review and perspective on industry high-temperature heat pumps. Renew Sustain Energy Rev 2022;161:112106. https://doi.org/10.1016/J.RSER.2022.112106.
[12] Adamson KM, Walmsley TG, Carson JK, Chen Q, Schlosser F, Kong L, et al. High-temperature and transcritical heat pump cycles and advancements: a review. Renew Sustain Energy Rev 2022;167:112798. https://doi.org/10.1016/J.RSER.2022.112798.
[13] Bamigbetan O, Eikevik TM, Nekså P, Bantle M. Review of vapour compression heat pumps for high temperature heating using natural working fluids. Int J Refrig 2017;80:197–211. https://doi.org/10.1016/J.IJREFRIG.2017.04.021.
[14] Chua KJ, Chou SK, Yang WM. Advances in heat pump systems: a review. Appl Energy 2010;87:3611–24. https://doi.org/10.1016/J.APENERGY.2010.06.014.
[15] Mateu-Royo C, Arpagaus C, Mota-Babiloni A, Navarro-Esbrí J, Bertsch SS. Advanced high temperature heat pump configurations using low GWP refrigerants for industrial waste heat recovery : a comprehensive study. Energy Convers Manag 2021;229. https://doi.org/10.1016/j.enconman.2020.113752.
[16] Schlosser F, Jesper M, Vogelsang J, Walmsley TG, Arpagaus C, Hesselbach J. Large-scale heat pumps: applications, performance, economic feasibility and industrial integration. Renew Sustain Energy Rev 2020;133:110219. https://doi.org/10.1016/j.rser.2020.110219.
[17] Kaida T, Sakuraba I, Hashimoto K, Hasegawa H. Experimental performance evaluation of heat pump-based steam supply system. 9th Int. Conf. Compressors their Syst. 2015. https://doi.org/10.1088/1757-899X/90/1/012076.
[18] Mateu-Royo C, Mota-Babiloni A, Navarro-Esbrí J. Semi-empirical and environmental assessment of the low GWP refrigerant HCFO-1224yd(Z) to replace HFC-245fa in high temperature heat pumps. Int J Refrig 2021;127:120–7. https://doi.org/10.1016/J.IJREFRIG.2021.02.018.

[19] Wu D, Hu B, Wang RZ, Fan H, Wang R. The performance comparison of high temperature heat pump among R718 and other refrigerants, vol. 154; 2020. https://doi.org/10.1016/j.renene.2020.03.034.

[20] Frate GF, Ferrari L, Desideri U. Analysis of suitability ranges of high temperature heat pump working fluids. Appl Therm Eng 2019;150:628–40. https://doi.org/10.1016/j.applthermaleng.2019.01.034.

[21] Höbberg M, Berntsson T. Non-azeotropic mixtures as working fluids in two-stage economizer-type heat pumps. Int J Refrig 1994;17:417–29. https://doi.org/10.1016/0140-7007(94)90077-9.

[22] Garimella S, Milkie J, Macdonald M. Condensation of zeotropic mixtures of low-pressure hydrocarbons and synthetic refrigerants. Int J Heat Mass Tran 2020;162:120301. https://doi.org/10.1016/J.IJHEATMASSTRANSFER.2020.120301.

[23] Zühlsdorf B, Jensen JK, Cignitti S, Madsen C, Elmegaard B. Analysis of temperature glide matching of heat pumps with zeotropic working fluid mixtures for different temperature glides. Energy 2018;153:650–60. https://doi.org/10.1016/j.energy.2018.04.048.

[24] Heberle F, Preißinger M, Brüggemann D. Zeotropic mixtures as working fluids in Organic Rankine Cycles for low-enthalpy geothermal resources. Renew Energy 2012;37:364–70. https://doi.org/10.1016/J.RENENE.2011.06.044.

[25] Marcoberardino G Di, Invernizzi CM, Iora P, Ayub A, Bona D Di, Chiesa P, et al. Experimental and analytical procedure for the characterization of innovative working fluids for power plants applications. Appl Therm Eng 2020;178:115513. https://doi.org/10.1016/j.applthermaleng.2020.115513.

[26] Crespi F, Rodríguez de Arriba P, Sánchez D, Ayub A, Di Marcoberardino G, Invernizzi CM, et al. Thermal efficiency gains enabled by using CO2 mixtures in supercritical power cycles. Energy 2022;238:121899. https://doi.org/10.1016/J.ENERGY.2021.121899.

[27] Zühlsdorf B, Jensen JK, Elmegaard B. Heat pump working fluid selection—economic and thermodynamic comparison of criteria and boundary conditions. Int J Refrig 2019;98:500–13. https://doi.org/10.1016/J.IJREFRIG.2018.11.034.

[28] Cao Y, Dhahad HA, Mohamed AM, Anqi AE. Thermo-economic investigation and multi-objective optimization of a novel enhanced heat pump system with zeotropic mixture using NSGA-II. Appl Therm Eng 2021;194:116374. https://doi.org/10.1016/j.applthermaleng.2020.116374.

[29] Huang X, Zhang J, Haglind F. Experimental analysis of condensation of zeotropic mixtures from 70°C to 90°C in a plate heat exchanger. Int J Refrig 2022. https://doi.org/10.1016/J.IJREFRIG.2022.01.029.

[30] Illán-Gómez F, Sena-Cuevas VF, García-Cascales JR, Velasco FJS. Analysis of the optimal gas cooler pressure of a CO2 heat pump with gas bypass for hot water generation. Appl Therm Eng 2021;182:116110. https://doi.org/10.1016/J.APPLTHERMALENG.2020.116110.

[31] Vuppaladadiyam AK, Antunes E, Vuppaladadiyam SSV, Baig ZT, Subiantoro A, Lei G, et al. Progress in the development and use of refrigerants and unintended environmental consequences. Sci Total Environ 2022;823:153670. https://doi.org/10.1016/J.SCITOTENV.2022.153670.

[32] Höhler F, Deschermeier R, Rehfeldt S, Klein H. Gas solubilities of carbon dioxide in methanol, acetone, mixtures of methanol and water, and mixtures of methanol and acetone. Fluid Phase Equil 2018;459:186–95. https://doi.org/10.1016/J.FLUID.2017.12.004.

[33] Ramírez-Ramos GE, Zgar Y, Salavera D, Coulier Y, Ballerat-Busserolles K, Coronas A. Vapor-liquid equilibrium, liquid density and excess enthalpy of the carbon dioxide+acetone mixture: experimental measurements and correlations. Fluid Phase Equil 2021;532:112915. https://doi.org/10.1016/J.FLUID.2020.112915.

[34] Moreira-Da-Silva RJB, Salavera D, Coronas A. Modelling of CO2/acetone fluid mixture thermodynamic properties for compression/resorption refrigeration systems. IOP Conf Ser Mater Sci Eng 2019;595:012030. https://doi.org/10.1088/1757-899X/595/1/012030. IOP Publishing.

[35] Kondou C, Koyama S. Thermodynamic assessment of high-temperature heat pumps using low-GWP HFO refrigerants for heat recovery. Int J Refrig 2015;53:126–41. https://doi.org/10.1016/j.ijrefrig.2014.09.018.

[36] Bamigbetan O, Eikevik TM, Nekså P, Bantle M, Schlemminger C. Experimental investigation of a prototype R-600 compressor for high temperature heat pump. Energy 2019;169:730–8. https://doi.org/10.1016/J.ENERGY.2018.12.020.

[37] Jensen JK, Ommen T, Markussen WB, Reinholdt L, Elmegaard B. Technical and economic working domains of industrial heat pumps: Part 2 - ammonia-water hybrid absorption-compression heat pumps. Int J Refrig 2015;55:183–200. https://doi.org/10.1016/j.ijrefrig.2015.02.011.

[38] Illán-Gómez F, Sena-Cuevas VF, García-Cascales JR, Velasco FJS. Experimental and numerical study of a CO2 water-to-water heat pump for hot water generation. Int J Refrig 2021;132:30–44. https://doi.org/10.1016/J.IJREFRIG.2021.09.020.

[39] ASHRAE. ASHRAE handbook—HVAC systems and equipment. SI Edition; 2020.

[40] Xia J, Wang J, Zhang G, Lou J, Zhao P, Dai Y. Thermo-economic analysis and comparative study of transcritical power cycles using CO2-based mixtures as working fluids. Appl Therm Eng 2018;144:31–44. https://doi.org/10.1016/J.APPLTHERMALENG.2018.08.012.

[41] Gui X, Tang Z, Fei W. Solubility of CO2 in alcohols, glycols, ethers, and ketones at high pressures from (288.15 to 318.15) K. J Chem Eng Data 2011;56:2420–9. https://doi.org/10.1021/JE101344V.

[42] Chen J, Wu W, Han B, Gao L, Mu T, Liu Z, et al. Phase behavior, densities, and isothermal compressibility of CO 2 + pentane and CO 2 + acetone systems in various phase regions. 2003. https://doi.org/10.1021/je034087q.

[43] Standards E. BS EN 378-1:2016+A1. Refrigerating systems and heat pumps. Safety and environmental requirements Basic requirements, definitions, classification and selection criteria. 2020.

[44] Poling BE, Prausnitz JM, O'Connel JP. The properties of gases and liquids. fifth ed.. 2001. New York.

[45] Lemmon EW, Bell IH, Huber ML, McLinden MO. NIST standard reference database 23: reference fluid thermodynamic and transport properties-REFPROP, version 10.0. Gaithersburg: National Institute of Standards and Technology, Standard Reference Data Program; 2018.

[46] Anthropogenic and natural radiative forcing. Clim Chang. Phys sci basis work gr I contrib to fifth. Assess Rep Intergov Panel Clim Chang 2013:659–740. https://doi.org/10.1017/CBO9781107415324.018. 2013;9781107057999.

[47] EU. Regulation (EU) No 517/2014 of the European parliament and of the council of 16 April 2014 on fluorinated greenhouse gases and repealing regulation (EC) No 842/2006. 2014. L150/195e230. n.d.

[48] UNEP. Handbook for the Montreal protocol on substances that deplete the ozone layer. eleventh ed. 2017.

[49] National Fire Protection Association. Nfpa 704 - standard system for the identification of the hazards of materials for emergency response, vol. 24; 2007.

[50] ASHRAE. Standard 34-safety standard for refrigeration systems and designation and classification of refrigerants. 2016.

[51] Zühlsdorf B, Jensen JK, Elmegaard B. Heat pump working fluid selection—economic and thermodynamic comparison of criteria and boundary conditions. Int J Refrig 2019;98:500–13. https://doi.org/10.1016/j.ijrefrig.2018.11.034.

[52] Traub P, Stephan K. Phase equilibria of the system CO2 -Water-Acetone measured apparatus of the system with a new. Chem Eng Sci 1990;45:751–8.

[53] Song Q, Wang D, Shen J, Zhao Y, Gong M. Flow condensation pressure drop characteristics of zeotropic mixtures of tetrafluoromethane/ethane: experimental and analytical investigation. Int J Heat Mass Tran 2022:182. https://doi.org/10.1016/j.ijheatmasstransfer.2021.122045.

[54] Wang L, Jiao P, Dang C, Hihara E, Dai B. Condensation heat and mass transfer characteristics of low GWP zeotropic refrigerant mixture R1234yf/R32 inside a horizontal smooth tube: an experimental study and non-equilibrium film model development. Int J Therm Sci 2021;170:107090. https://doi.org/10.1016/j.ijthermalsci.2021.107090.

[55] Zühlsdorf B, Meesenburg W, Ommen TS, Thorsen JE, Markussen WB, Elmegaard B. Improving the performance of booster heat pumps using zeotropic mixtures. Energy 2018;154:390–402. https://doi.org/10.1016/j.energy.2018.04.137.

[56] Lorenz H. Beiträge zur Beurteilung von Kühlmaschinen. Zeitschrift Des VDI 1894;38:62–8.

[57] Todd Reaves J, Griffith AT, Roberts CB. Critical properties of dilute carbon dioxide + entrainer and ethane + entrainer mixtures. J Chem Eng Data 1998;43:683–6. https://doi.org/10.1021/je9702753.

[58] Han F, Xue Y, Tian Y, Zhao X, Chen L. Vapor-liquid equilibria of the carbon dioxide + acetone system at pressures from (2.36 to 11.77) MPa and temperatures from (333.15 to 393.15) K. J Chem Eng Data 2005;50:36–9. https://doi.org/10.1021/je049887v.

[59] Bamberger A, Maurer G. High-pressure (vapour + liquid) equilibria in (carbon dioxide + acetone or 2-propanol) at temperatures from 293 K to 333 K. J Chem Thermodyn 2000;32:685–700. https://doi.org/10.1006/jcht.1999.0641.

[60] Fábián B, Horvai G, Idrissi A, Jedlovszky P. Vapour-liquid equilibrium of acetone-CO2 mixtures of different compositions at the vicinity of the critical point. J CO2 Util 2019;34:465–71. https://doi.org/10.1016/j.jcou.2019.07.001.

[61] Chen J, Wu W, Han B, Gao L, Mu T, Liu Z, et al. Phase behavior, densities, and isothermal compressibility of CO2 + pentane and CO2 + acetone systems in various phase regions. J Chem Eng Data 2003;48:1544–8. https://doi.org/10.1021/je034087q.

[62] Fukuda S, Kondou C, Takata N, Koyama S. Low GWP refrigerants R1234ze(E) and R1234ze(Z) for high temperature heat pumps. Int J Refrig 2014;40:161–73. https://doi.org/10.1016/j.ijrefrig.2013.10.014.

[63] Violette M, Cyril P, Schiffman J. Data driven predesign tool for small scale centrifugal compressor in refrigeration. J Eng Gas Turbines Power 2018;140.

[64] Schiffmann J, Kontomaris K, Arpagaus C, Bless F, Bertsch S. Scale limitations of gas bearing supported turbocompressors for vapor compressoin cycles. Int J Refrig 2020;109:92–104.